LA-UR- 04-0267

**Title:** Electronic Structure of delta-Pu and PuCoGa5 from Photoemission and the Mixed Level Model

**Author(s):** John Joyce, MST-10; John Wills, T-1; Tomasz Durakiewicz, Martin Butterfield, Elzbieta Guziewicz, John Sarrao, MST-10; Aloysius Arko, David P. Moore, NMT; Luis Morales, NMT-16; Olle Eriksson, Uppsala University

LOS ALAMOS NATIONAL LABORATORY
3 9338 00995 2895

# Los Alamos
NATIONAL LABORATORY

# Electronic Structure of δ-Pu and PuCoGa₅ from Photoemission and the Mixed Level Model

John J. Joyce, John M. Wills[1], Tomasz Durakiewicz, Elzbieta Guziewicz, Martin T. Butterfield,
Aloysius J. Arko, David P. Moore[2], John, L. Sarrao, Luis A. Morales[2] and Olle Eriksson[3]
Condensed Matter & Thermal Physics Group, Los Alamos National Laboratory
Los Alamos, NM 87545, U.S.A.
[1]Theoretical Division, LANL
[2]Nuclear Materials Technology Division, LANL
[3]Department of Physics, Uppsala University, Box 530, Sweden

## ABSTRACT

The electronic structure of δ-phase Pu metal and the Pu-based superconductor PuCoGa₅ is explored using photoelectron spectroscopy and a novel theoretical scheme. Excellent agreement between calculation and experiment defines a path forward for understanding electronic structure aspects of Pu-based materials. The photoemission results show two separate regions of 5f electron spectral intensity, one at the Fermi energy and another centered 1.2 eV below the Fermi level. A comparison is made between the photoemission data and five computational schemes for δ-Pu. The results for δ-Pu and PuCoGa₅ indicate 5f electron behavior on the threshold between localized and itinerant and a broader framework for understanding the fundamental electronic properties of the Pu 5f levels in general within two configurations, one localized and one itinerant.

## INTRODUCTION

Within the actinide series, Pu occupies the position between the clearly hybridized 5f states of uranium and clearly localized 5f states of americium. Pu defines the localized/itinerant boundary for the 5f electrons in the actinides. The role of the 5f electrons in bonding and hybridization is intimately intertwined with the wide range of ground state properties found in actinide materials including enhanced mass, magnetism, superconductivity, as well as spin and charge density waves. There have been several recent papers reporting photoemission (PES) [1-4] and electronic structure calculations [5-9] for the fcc δ-phase of Pu metal. A classic failure of density functional theory (DFT) within the local density approximation (LDA) or generalized gradient approximation (GGA) is observed in the case of δ-Pu with the volume from LDA falling some 25% short of the experimental value in the largest discrepancy to date in DFT for a crystal.

To accommodate the large volume of the delta phase of Pu metal, there have been magnetically ordered electronic structures proposed [5] which essentially remove some of the 5f electrons from participating in bonding thus reducing the contribution to chemical bonding and increasing the volume. Although computationally enlightening, there is no experimental evidence for magnetism in δ-Pu. Another approach used for δ-Pu is the dynamical mean field theory (DMFT) which considers many-body effects, finds evidence for strong correlations and may offer additional promise with further development [6].

There are currently four computational frameworks to describe the electronic structure of PuCoGa₅ three within the framework of DFT [10-12] and the mixed level model (MLM) [13]. The theoretical efforts for PuCoGa₅ are following the path set forth in δ-Pu, with conventional

DFT pushing the 5f-electron intensity up against the Fermi level or magnetic solutions which serve to redistribute some of the Pu 5f intensity below the Fermi level ($E_F$). For PuCoGa$_5$, as in δ-Pu, there is no experimental evidence for magnetism [14]. PuCoGa$_5$ has a Curie-Weiss susceptibility while δ-Pu is a temperature independent paramagnet. However, the magnetic solutions for both δ-Pu and PuCoGa$_5$ provide valuable insight into the electronic structure. The agreement between photoelectron spectroscopy (PES) and calculation is improved in the magnetic calculations compared with conventional DFT calculations without magnetism. The magnetic state, by removing 5f electrons from a bonding configuration effectively localizes f-electrons and thus removes them from the Fermi energy and so provides the needed spectral intensity away from the Fermi level to match the PES results.

The link between δ-Pu metal and PuCoGa$_5$ is strong and follows the same path as the family of Ce-based heavy fermion-superconductors (CeMIn$_5$, M=Co, Rh, Ir) having the cubic CeIn$_3$ as the root crystal structure [15]. Here we have δ-Pu as the parent cubic phase structure with Ga substituting on the face centers to form PuGa$_3$ and insertion of the CoGa$_2$ layer into the cubic structure to form PuCoGa$_5$ in the tetragonal phase. With the discovery of superconductivity in PuRhGa$_5$ [16] it does indeed seem reasonable that the PuMGa$_5$ family of compounds is following systematics much like the CeMIn$_5$ family of superconducting compounds.

Understanding the nature of the 5f electrons is central to understanding the electronic properties of Pu-based materials. In this paper we present experimental evidence for the Pu 5f electrons in two configurations, one well removed from $E_F$ and one directly at $E_F$ in a peak consistent with narrow band characteristics of other actinides. Additionally, the MLM calculations presented showing remarkable agreement with the PES data where the Pu 5f electrons exist in two configurations, one localized and one itinerant.
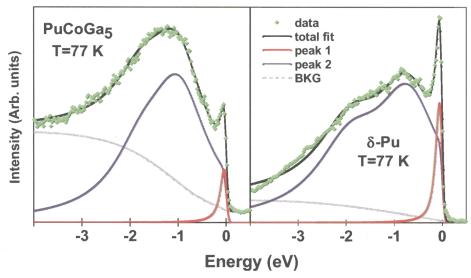

**EXPERIMENTAL DETAILS**

The PES data was collected using the Laser Plasma Light Source (LPLS) at Los Alamos National Laboratory. The LPLS is a tunable light source for transuranic photoemission with a photon energy range (hv) of 27 to 140 eV and uses a discharge lamp for high resolution and fixed photon energies (hv=21.2, 40.8 and 48.4 eV). Here we present only data taken at hv=40.8 eV. At this energy the cross-section for the Pu 5f and the Pu 6d levels are nominally equal and the cross-section for the Co 3d level is also comparable [17]. We have previously shown that at this energy for δ-Pu, a calculation using full initial and final state matrix element effects compares very well with a calculated density of states (DOS) [9]. The PuCoGa$_5$ sample was a single crystal grown by the flux growth method and the δ-Pu sample was polycrystalline stabilized with 1.7 atomic percent Ga in the Pu. The measurement temperature was 77 K and the experimental resolution was 60 meV for δ-Pu and 75 meV for PuCoGa$_5$. The samples were cleaned by laser ablation and free of contamination as determined by the full valence band spectra.

**DISCUSSION**

In figure 1 we show PES data for PuCoGa$_5$ and δ-Pu metal. The data are the green diamonds while the lines are fits to the data. The black line is the total fit, the gray line is the inelastic scattering background function while the red and blue lines are the first and second fitted peaks.

The fits are essentially the same for both materials. The second peak (blue line) is actually two overlapping peaks. Two points are important to observe in this data. First, there is a peak at the Fermi level having a width on the occupied side of $E_F$ of ~100 meV. Second, there is a peak centered ~1.2 eV below $E_F$ which contains the majority of the spectral intensity. In δ-Pu this second peak is primarily of Pu 5f character while in PuCoGa$_5$ this peak is a combination of Pu 5f and Co 3d character and accounts for the difference in intensities between the $E_F$ peak and the 1.2 eV peak in the two materials. We use a Lorentzian lineshape for the natural linewidth (Doniach-Sunjic lineshape was not required) convoluted with a Gaussian for the instrument resolution and a 77 K Fermi function to fit the data [18]. The partitioning of the PES spectral intensity (and consequently by cross-section arguments the Pu 5f levels) into two distinct regions is a fundamental characteristic of both δ-Pu and PuCoGa$_5$ as well as several other Pu compounds.
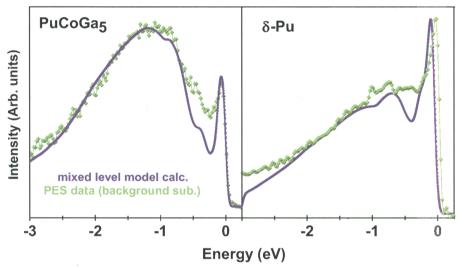


**Figure 1.** Photoemission data for PuCoGa$_5$ and δ-Pu at hν=40.8 eV and T=77 K (green diamonds). The black line is the sum of the fitted components while the red line is the first peak, the blue line a second feature comprised of two broader peaks and the gray line is a background function.

The PES data along with a MLM calculation for both δ-Pu and PuCoGa$_5$ is shown in figure 2. There is very good agreement between the data and the MLM calculation for both materials. The basis of the MLM is a partitioning of the electron density into localized and delocalized parts, minimizing the total energy (including a correlation energy associated with localization) with respect to the partitioning. The total energy of PuCoG$_5$, and of δ-Pu becomes minimized for an atomic 5f$^4$ configuration with roughly one 5f-electron in a delocalized Bloch state. The four localized 5f electrons couple into a singlet, a many-body effect that is not accounted for within a single-particle picture. The hybridization between the conduction band states and the localized f-states (here a four electron multiplet state) is a key interaction needed to produce an accurate theoretical spectrum. The hybridization matrix element is calculated from the width of the 5f-resonance which is proportional to the 5f electron wavefunction at the muffin-tin sphere. This value indicates that spin and orbital couplings within the 5f shell are important in this system. In addition to a broadening of the 5f-level, the hybridization matrix elements cause a reduction in

the spectral weight. Hence the hybridization results in a broadening and a shift of the spectral weight. The good agreement between the PES data and the MLM calculation for a tetragonal ternary Pu compound and a cubic Pu metal phase demonstrates the broad applicability of this approach to the electronic structure of Pu materials. Both the PES and the MLM identify the Pu 5f electrons in two configurations, one localized and one itinerant. The itinerant nature of the $E_F$ peak in PES is confirmed by photon energy dependence as shown in Ref. [9] for δ-Pu and Ref. [13] for $PuCoGa_5$.
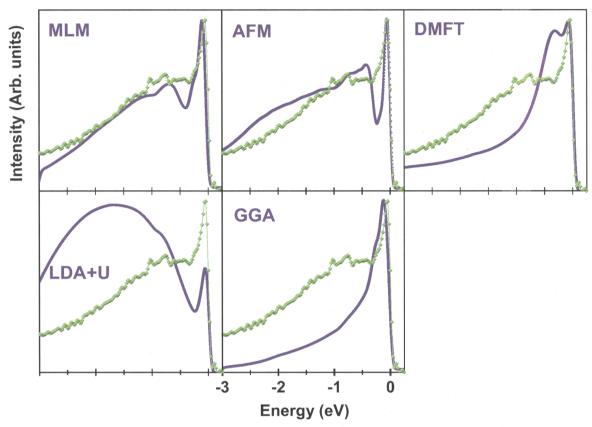
For comparing calculations with PES data we process all calculations as follows; 1) the DOS is multiplied by a 77 K Fermi function, 2) the resulting DOS is then Lorentzian broadened by an energy dependent photohole lifetime width which depends on $E^2$ with respect to $E_F$ (consistent with Fermi liquid theory), 3) the resulting DOS is finally convoluted with a Gaussian instrument response function.



**Figure 2.** Photoemission data for $PuCoGa_5$ and δ-Pu at hν=40.8 eV and T=77 K (green diamonds) compared with mixed level model calculations (blue lines).

As indicated in the introduction there have been several computational approaches for δ-Pu in the last four years. In figure 3 we compare five different calculations to the PES data for δ-Pu. All of the calculations have been processed for PES comparison as described above for the MLM. The GGA calculation is from Ref. [3], the antiferromagnetic (AFM) calculation closely follows that of Ref. [5], the DMFT calculation is from Ref. [6], the LDA calculation with an explicit Coulomb correlation effect (LDA+U) is from Ref. [7] and the MLM calculation is from Ref. [9]. It is observed from this comparison that only the MLM and AFM calculations give reasonable agreement with the PES data. The LDA+U calculation shows far too much intensity well below the Fermi level while the DMFT calculation does not show enough separation between the peak at $E_F$ and the next spectral feature. Not surprisingly, The GGA calculation is fundamentally at odds with the PES data with a one-electron approach unable to account for the complex electronic structure of δ-Pu. While the AFM calculation shows reasonable agreement with PES, there is no known magnetism in δ-Pu and this structure would be inconsistent with known neutron scattering, magnetic susceptibility and recent nuclear magnetic resonance (NMR) data [19]. Even within the most recent variant of the AFM calculation, the disordered local moment approach the computational results would be inconsistent with the experimental results

for δ-Pu. The analysis of figure 3 leads one to the conclusion that the MLM is the most suitable computational approach for dealing with δ-Pu. Since this model also works well for PuCoGa$_5$ this would seem to be an important innovation in the understanding of Pu electronic structure. The results are qualified by the realization that PES is only one experimental tool for exploring Pu materials, yet PES is a very direct probe of the electronic structure and offers one of the single best experimental probes into the complexity of correlated electron physics.



**Figure 3.** Photoemission data for δ-Pu at hν=40.8 eV and T=77 K (green diamonds) compared against five computational models (blue lines) for δ-Pu. The model calculations have been processed for the Fermi function, instrument resolution and photohole lifetime broadening.

## CONCLUSION

The PES data for δ-Pu and PuCoGa$_5$ gives solid evidence of the Pu 5f electrons occurring in two configurations, one itinerant and being located near the Fermi level, the other localized and centered ~1.2 eV below E$_F$. The MLM calculation shows this same Pu 5f arrangement, with one 5f electron being itinerant and the other four 5f electrons being localized. The agreement between PES and the MLM for δ-Pu and PuCoGa$_5$ is very good and the best of the five computational schemes recently published. We have presented reliable PES data in good agreement with theoretical calculations. These calculations also yield volumes in agreement with experimental values and no long range magnetic order. Using PES data and MLM calculations a reasonable approach is developing towards an understanding of the complex electronic structure of Pu-based materials.

## ACKNOWLEDGMENTS

## REFERENCES

1. L. Havela *et al.*, Phys. Rev. B **65**, 235118 (2002); T. Gouder *et al.*, Euro Phys. Lett. **55**, 705 (2001); T. Almeida *et al.*, Surf. Sci. **287**, 141 (1993).
2. J. Terry, *et al.*, Surface Science **499**, L141 (2002).
3. A.J. Arko *et al.*, Phys. Rev. B **62**, 1773 (2000).
4. J.J. Joyce *et al.*, Surf. and Interface Analysis **26**, 121 (1998).
5. Per Soderlind, Alex Landa, and Babak Sadigh, Phys. Rev. B **66**, 205109 (2002).
6. S.Y. Savrasov, G. Kotliar and E. Abrahams, Nature **410**, 793 (2001).
7. J.Bouchet, *et al.*, J. Phys. - Cond. Matter, **12**, 1723 (2000).
8. O. Eriksson *et al.*, J. Alloys and Compounds **287**, 1 (1999).
9. J.M. Wills *et al.*, J. Elect. Spectr. and Related Phenom. accepted (2003), also arXiv server (cond-mat/0307767).
10. A. Szajek and J.A. Morkowski, J. Phys. Cond. Matt. **15**, L155 (2003).
11. I. Opahle and P.M. Oppeneer, Phys. Rev. Lett. **90**, 157001 (2003).
12. T. Maehira *et al.*, Phys. Rev. Lett. **90**, 207007 (2003).
13. J.J. Joyce *et al.*, Phys. Rev. Lett. **91**, 176401 (2003).
14. J.L. Sarrao *et al.*, Nature **420**, 297 (2002).
15. H. Hegger *et al.*, Phys. Rev. Lett. **84**, 4986 (2000); C. Petrovic *et al.*, Europhys. Lett. **53**, 354 (2001); C. Petrvic *et al.*, J. Phys.: Condens. Matter. **13**, L337 (2001).
16. F. Wastin, *et al.*, J. Phys. : Condens. Matter. **15**, S2279 (2003).
17. J.J. Yeh and I. Lindau, Atomic Data and Nuclear Data Tables, **32**, 1 (1985).
18. J.J. Joyce *et al.*, Phys. Rev. B **54**, 17515 (1996).
19. N. Curro, Mater. Research Society, Fall 2003 meeting and this proceedings.